An Optimized Blockwise Nonlocal Means Denoising Filter for 3-D Magnetic Resonance Images

Ngoc Phuc Nguyen

***Abstract*— Removing noise while keeping the integrity of relevant image information has been a huge challenge in image processing. Most classical denoising filters restore the intensity value of image elements by averaging neighboring pixels or voxels. This technique achieves good performance in homogeneous areas, however, with areas containing significant changes of intensity, the nonlocal (NL)-means filter gains huge advantages since it uses the redundancy of information in the image to remove noises. In this paper, the method proposed is based on a 3-D optimized block-wise version of the NL means filter with several improvements to reduce computational burden. In this report, a fully automated and optimized version of NL-means filter is presented. Beside the implementation of the filter, an automatic tuning of the smoothing parameter and a selection of the most relevant voxels in the searching area are integrated to improve denoising capability and running time. For validation, the synthetic datasets generated with BrainWeb (Collins, et al., 1998) is used for evaluating the performance of the optimized filter along with the traditional 2-D nonlocal means filter.**

***Index Terms*— Image denoising, image enhancement, nonlocal means filters, medical images.**

Manuscript written Dec 2, 2020; revised Dec 6, 2020. *Asterisk indicates author*.

*Ngoc Phuc Nguyen is with Concordia University.

I. INTRODUCTION

QUANTITATIVE imaging heavily relies on denoising processes to pave the way for robust post-processing. However, the main problem of denoising is that removing noises could destroy noise-sensitive information of images. This is also true for processing medical images when ultrasound images or magnetic resonance images (MRI) are highly sensitive with noises. Especially, MR images constantly contain weak signals which are usually fluctuating around noise levels. In addition, rapid developments of technology permit collecting larger cohorts of 3-D data and longer image sequences. That means human intervention is no longer feasible to process huge datasets and a complex algorithm for medical image processing is required. For effectiveness, the novel filter has to have a capability to process a wide range of image quantities and to tune its parameters for different processing contexts. The nonlocal (NL) means filter was first introduced by Buades *et al*. [1] for 2-D image denoising. The extended version to 3-D images in this report mainly focuses on the contributions of 1) an automatic tuning of smoothing parameter; 2) a selection of the most relevant voxels for NL-means computation; 3) a block-wise implementation. These contributions allow the optimized filter to work independently and significantly reduce the computational time, which is the critical drawback of classical NL-means filters.

Section II presents several techniques in image restoration. Section III introduces the contributions to the existing 3-D NL means filter in details. Section IV shows the performance of optimized nonlocal mean denoising filter with the 2-D classical method on different BrainWeb dataset such as T1, T2 MRI with protocol ICBM and T2 with protocol AI of a patient with multiple sclerosis lesions (MSL).

II. STATE-OF-THE-ART

A. General Overview

Many denoising approaches for preserving edges of images have been proposed. Some popular methods can be named as Bayesian approaches [7] which use probability to estimate the corrupted data, PDE-based approaches [3], [4], [8], [9], regression estimation use gradient descent to find approximately correct values for restoration [10], adaptive smoothing [11], wavelet-based methods transform images to frequency domain [12] - [14].

2D domain and later on extended to 3-D medical data such as AD [34], [35], TV [36], bilateral filtering and variants [37], wavelet-based filtering [38] - [42], and hybrid filters [43], [44]. Currently, more and more machine learning (ML) approaches have been introduced such as modeling NL pairwise interactions from training data [30] or comparing the medical data with a library of natural image patches [31], [32].

B. Introduction of the NL-Means Filter

Nonlinear means filters recover the intensity value of image elements by taking the average of each neighborhood value (so-called box filtering [45]). In practice, this filter does outperform the Gaussian filters, which restore the image elements by weighting its neighborhood according to the distance between the neighborhood elements and the restored element under study. However, the Gaussian filter is a data-independent filter which operates with fixed parameters. This kind of filter is very efficient in homogeneous areas. However, in some areas such as edges or small textures, the structures of interest can be blurred.

This rises the demand of data-dependent approaches, which automatically adjust the influence of the neighboring voxels

dissimilar to the image element under study. Recently, a novel idea that any natural image has redundancy has been proposed. This idea said that any voxel of the images has similar voxels which is not located in a spatial neighborhood. This was first introduced by Buades *et al*. in [1], the NL-means filter is based on this property. In this method, the voxels under study will be restored based on the intensity similarity of their neighborhoods but not by the average of them. This new NL recovery paradigm can both solve the two most important of a denoising algorithm which are 1) edge preservation since it does not blur the image information and 2) noises removal when noises could be eliminated when we increase samples of a similar element.

III. METHODS

In the report, we introduce the notations.

$u(x_i)$	Intensity observed at voxel x_i
V_i	Cubic search volume centered on voxel x_i of size $\|V_i\| = (2M+1)^3, M \in \mathbb{N}$
N_i	Cubic local neighborhood of x_i of size $\|N_i\| = (2d+1)^3, d \in \mathbb{N}$
$\boldsymbol{u}(N_i) = (u^1(N_i), \dots, u^{(\|N_i\|)}(N_i))^T$	Vector containing the intensity of N_i
$NL(u)(x_i)$	Restored value of voxel x_i
$w(x_i, x_j)$	Weight of voxel x_i when restoring $u(x_i)$

For the block-wise NL-means approach.

B_i	Block centered on x_i of size $\|B_i\| = (2\alpha+1)^3, \alpha \in \mathbb{N}$
$\boldsymbol{u}(B_i)$	Vector containing the intensity of block B_i
$\boldsymbol{NL}(u)(B_i)$	Vector containing the restored value of B_i
$w(B_i, B_j)$	Vector containing the intensity of N_i
$NL(u)(x_i)$	Restored value of voxel x_i
$w(x_i, x_j)$	Weight of voxel B_i when restoring the block $\boldsymbol{u}(B_i)$
B_{i_k}	Blocks centered on voxels x_{i_k} i-th $i_k = (k_1 n, k_2 n, k_3 n), (k_1, k_2, k_3) \in \mathbb{N}^3$ and n represents the distance between the centers of the blocks B_{i_k}

A. Nonlocal Means Filter

The formulation of the NL-means filter is the combination of the weight average of all the voxel intensities in an image area, this is the practical approach since the number of sample voxel need to be restricted into small areas.

$$NL(u)(x_i) = \sum_{x_i \in V_i} w(x_i, x_j) u(x_i) \tag{1}$$

Where $u(x_i)$ is the intensity of the voxel x_i and $w(x_i, x_j)$ is the amount of the intensity $u(x_i)$ needed for restoring x_i. In other words, the weight is decided based on the similarity of the local neighborhoods N_i and N_j of the voxels x_i and x_j under the limitation that $w(x_i, x_j) \in [0,1]$ and $\sum_{x_i \in \Omega^3} w(x_i, x_j) = 1$. Theoretically, each x_i voxel can look for the similarity to all voxel in image in order to recover information, however, for computational reason, each voxel under restoration is linked to a certain number of voxel in the search volume V_i which has size $(2M+1)^3$, centered at the voxel x_i.

The weight $w(x_i, x_j)$ is measured by taking the Euclidean distance of 2 neighborhoods of x_i and x_j, which are $\boldsymbol{u}(N_i)$ and $\boldsymbol{u}(N_j)$, respectively. This distance is then convolved with the Gaussian kernel and constrained by smoothing parameter h. The weight is defined as:

$$w(x_i, x_j) = \frac{1}{Z_i} e^{-\frac{\|\boldsymbol{u}(N_i) - \boldsymbol{u}(N_j)\|^2_{2,a}}{h^2}} \tag{2}$$

where Z_i is the normalization to ensure that $\sum_j w(x_i, x_j) = 1$, h acts as a controlling parameter of the exponential decay. When h is high, all the voxel x_j in V_i will have the same weight $w(x_i, x_j)$, hence, this leads to the restoration of x_i is the average of all voxel x_j in V_i. On the other hand, when h is low, only some of the voxel x_j in V_i will have significant weights and the other is 0. The restored image will be weak in smoothing since just some of the voxel x_j has the same similarity with x_i . The main problem of this NL-means filter is when we apply it on 3D images. The complexity of the algorithm is then the order of $\mathcal{O}((N(2M+1)\,(2d+1))^3)$. For a 3D MRI dataset of size 181 x 217 x 181 with smallest d = 1 and M = 5, It could take up to 6 hours to process the whole MRI sequence and this is unacceptable from the standpoint of denoising in medical field.

B. Improvement of the NL-Means Filter

1) Automatic tuning of the smoothing parameter h: according to [1] the h relies on the standard deviation of the noise σ, and for the 2-D scenario, h might be equal to 10σ. For the 3-D context, h needs to be adapted to an equivalent filter. The automatic tuning parameter h has the relationship that: $h = f(\sigma^2, |N_i|, \beta)$ where β is a constant.

The standard deviation of noise can be calculated by pseudo-residual ϵ_i as defined in [49] [50]. For each voxel x_i of the volume Ω^3, we take the intensities of six-neighborhood centered around voxel x_i which is located in two side following the x axis, the y axis and the z axis.

$$\epsilon_i = \sqrt{\frac{6}{7}}\left(u(x_i) - \frac{1}{6}\sum_{x_j \in P_i} u(x_j)\right) \tag{3}$$

The standard derivation of noise is defined as:

$$\hat{\sigma}^2 = \frac{1}{|\Omega^3|}\sum_{i \in \Omega^3} {\epsilon_i}^2. \tag{4}$$

For the weight assigned to x_i in V_i, the weight $w(x_i, x_j)$ is calculated by taking the normalized Euclidean distance L2 of x_i and x_j neighborhood.

$$\frac{1}{|N_i|}\left\|\boldsymbol{u}(N_i)-\boldsymbol{u}(N_j)\right\|_2^2=\frac{1}{|N_i|}\sum_{p=1}^{|N_i|}\left(u^p(N_i)-u^p(N_j)\right)^2 \quad (5)$$

Then, (2) equals to:

$$w(x_i,x_j)=\frac{1}{Z_i}e^{-\frac{\left\|\boldsymbol{u}(N_i)-\boldsymbol{u}(N_j)\right\|_2^2}{2\beta\hat{\sigma}^2|N_i|}} \quad (6)$$

According to [51, p. 21], β is close to 1 in case of Gaussian noise.

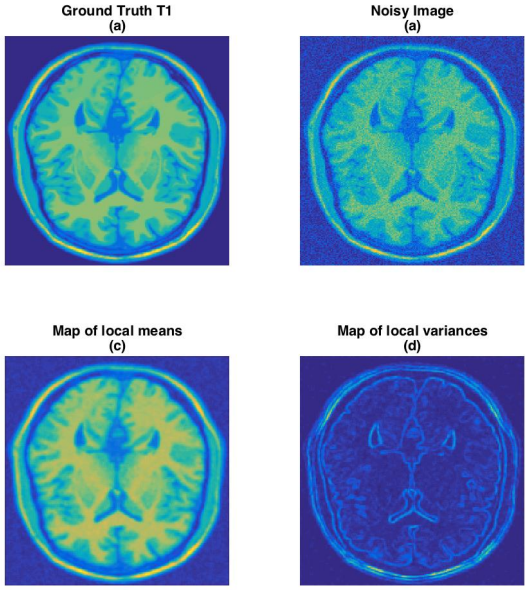

Figure 1 (a) Ground Truth image in T1 dataset, (b) noisy image with 9% Gaussian noise, (c) Map of the mean $\boldsymbol{u}(N_i)$ denoted $\overline{\boldsymbol{u}(N_i)}$, (d) Map of the variance of $\boldsymbol{u}(N_i)$ denoted as $Var\left(\boldsymbol{u}(N_i)\right)$.

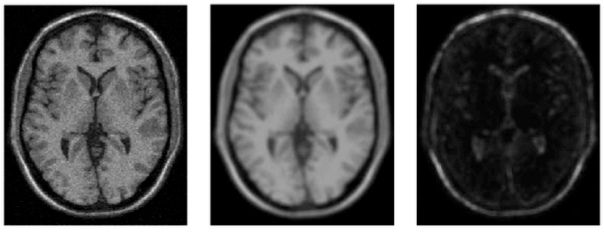

Figure 2 The map of local means (b) and map of the variances (c) in the main paper.

2) Voxel selection in the Search Volume: To reduce the computing time, Mahmoudi and Sapiro [52] have proposed an approach to select only the crucial x_i for restoration without the need of calculating the Euclidean distances between $u(N_i)$ and $u(N_j)$. The selection is based on the local mean and variance of $u(N_i)$ and $u(N_j)$. For the convenience, the map of local mean and local variance will be computed in advance to avoid repetitive calculation of the same neighborhood.

$$w(x_i,x_j)=\begin{cases}\frac{1}{Z_i}e^{-\frac{\left\|\boldsymbol{u}(N_i)-\boldsymbol{u}(N_j)\right\|_2^2}{2\beta\hat{\sigma}^2|N_i|}}, if\ \mu_1<\frac{\overline{\boldsymbol{u}(N_i)}}{\overline{\boldsymbol{u}(N_j)}}<\frac{1}{\mu_1}\ and\\ \qquad\qquad \sigma_1^2<\frac{Var\left(\boldsymbol{u}(N_i)\right)}{Var\left(\boldsymbol{u}(N_j)\right)}<\frac{1}{\sigma_1^2}\\ 0,\qquad otherwise\end{cases} \quad (7)$$

Where $\overline{\boldsymbol{u}(N_i)}$ and $Var\left(\boldsymbol{u}(N_i)\right)$ are the mean and the variance of local neighborhood N_i of voxel x_i.

IV. Materials

A. BrainWeb Database

1) To evaluate the performance of the filter, two MR image sequences with ICBM protocol are used. The dataset is called BrainWeb which has volume size = 181 x 217 x 181 and corrupted by a white Gaussian noise in different levels.

- T1 MR images were stimulated in different noise levels of 3%, 5%, 7%, and 9%.

2) T2-AI protocol with Multiple Sclerosis Lesions: In case of neurological diseases such as MS lesions, the damaging structure has a small size and is easily wiped out by the denoising method. With the 2-D traditional method it is hard to identify the small lesions while they are similar to noises.

- T2 AI images were stimulated in different noise levels of 3%, 5%, 7%, and 9%.

T2-AI images set are introduced to verify that the approach and its calibration are not only for the T1 MRI sequences.

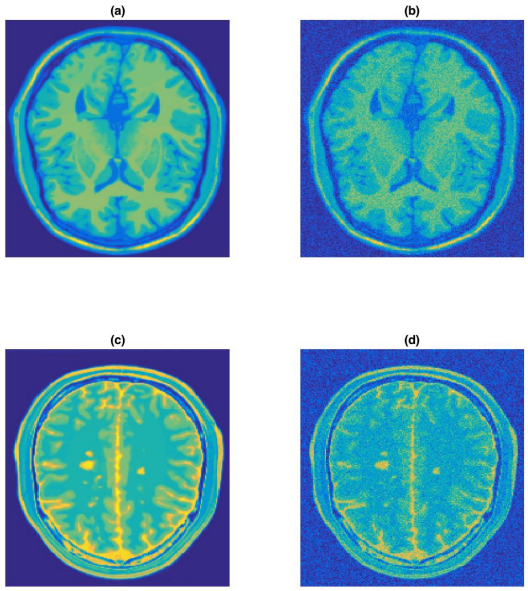

Figure 3 Synthetic data used for testing optimized NL means filter. Top: (a) ground truth of T1 images without any noise, and corrupted

version with 9% of Gaussian noise (b). Bottom: T2 images with MS lesions without noise (c), and corrupted with 9% Gaussian noise (d).

V. VALIDATION

For validation, the report will use the BrainWeb dataset to test the filter in different noise levels and compare with the result in the paper. The main method is using classical voxel wise nonlinear means filter with auto tuning smoothing parameter and voxel selection in the search volume.

In each experiment, the parameters are set with default values

- β is the constant in calculating h, $\beta = 1$
- M is the width of seaching volume, $|V_i| = (2M+1)^3, M = 5$
- d is the width of neiborhood, $|N_i| = (2d+1)^3, d = 1$
- μ_1 and σ_1^2 related to the thresholds in selecting voxel, $\mu_1 = 0.95, \sigma_1^2 = 0.5$

Since, in the paper, authors just apply the filter on the T2-BrainWeb with MS lesions. Hence, the comparison with the paper is just only on that case. Other testing cases are the comparison of noisy images and restored images.

1. T2 with MS lesions:

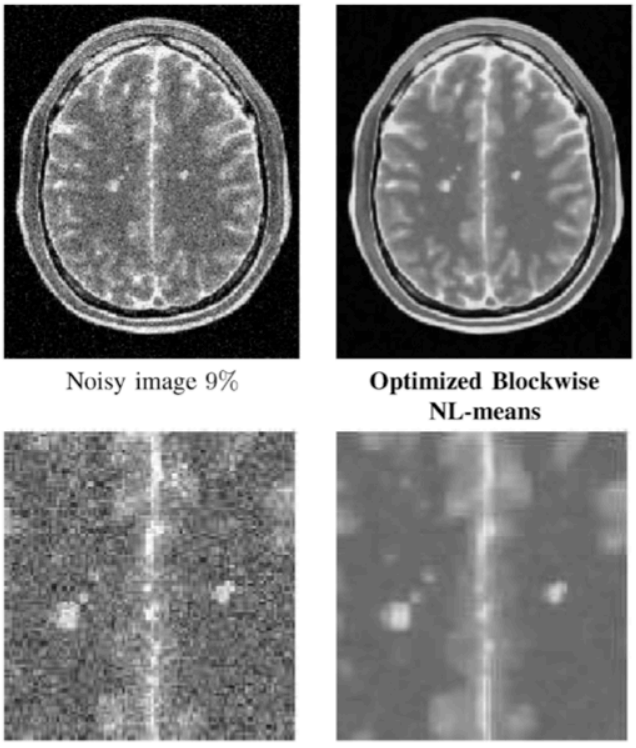

Figure 4 The restoration of T2 with MS lesion with 9% of Gaussian noise in the paper

For the implementation, it can be seen that the image restoration of the paper and the report is identical, take a look at the noises removed from the the noisy image, in the homogeneous areas, noises has been removed significantly and some of small interest structures are recovered. Ground truth is also provided to compare the result between the paper and the report.

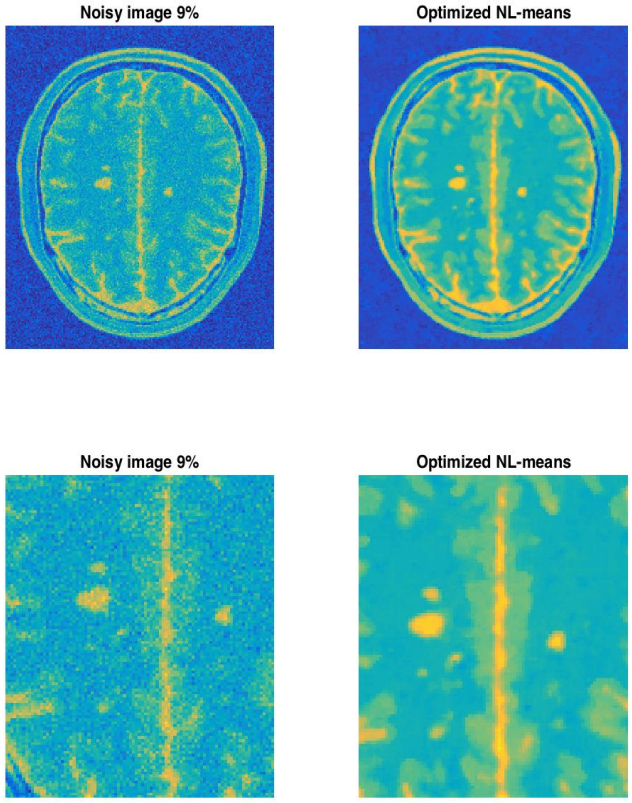

Figure 5 The restoration of T2 with MS lesion with 9% of Gaussian noise in the student report.

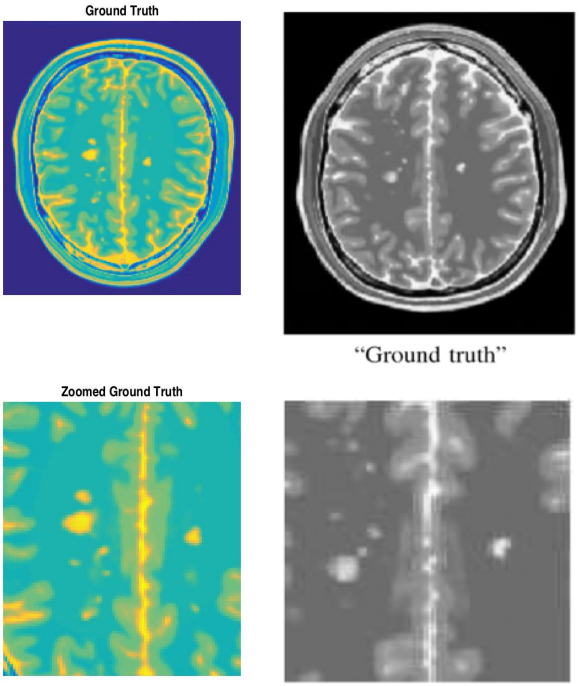

Figure 6 The T2 Ground truth with MS lesion with 9% of Gaussian noise in the student report and paper.

2. T1 with ICBM protocol ground truth at all noise levels.

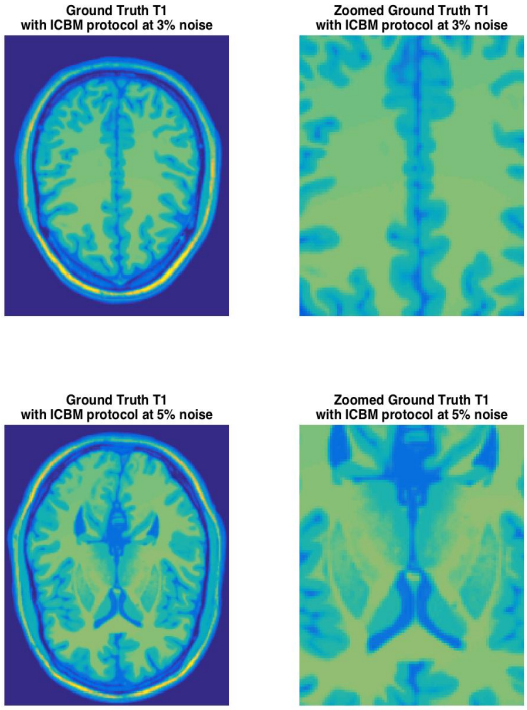

Figure 7 Ground truth of T1 with ICBM protocol at 3% and 5% noise added

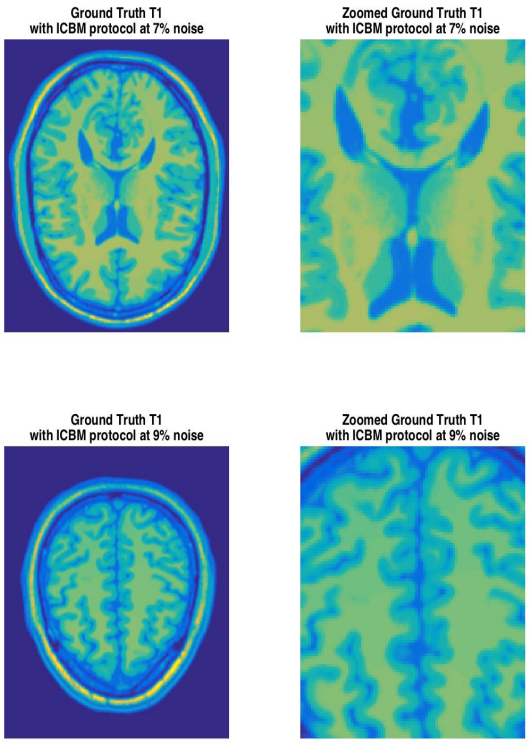

Figure 8 Ground truth of T1 with ICBM protocol at 7% and 9% noise added

3. T1 with ICBM protocol at 3% and 5% noise added and its restorations:

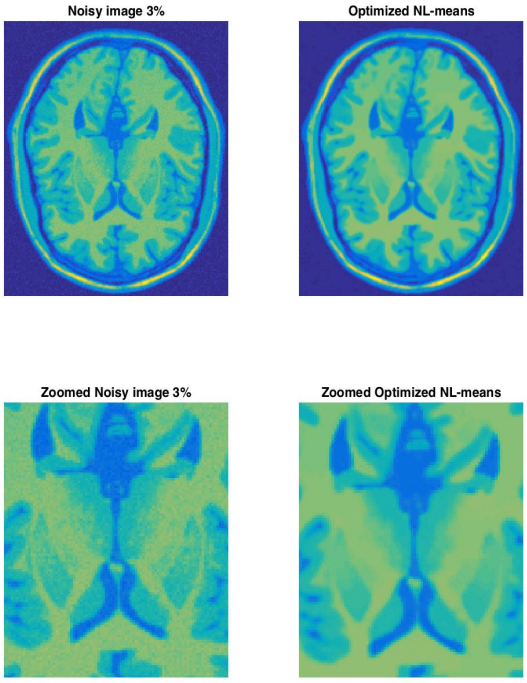

Figure 9 Noisy image with 3% noise added and its restoration, the image displayed is the slide 75th of the sequence.

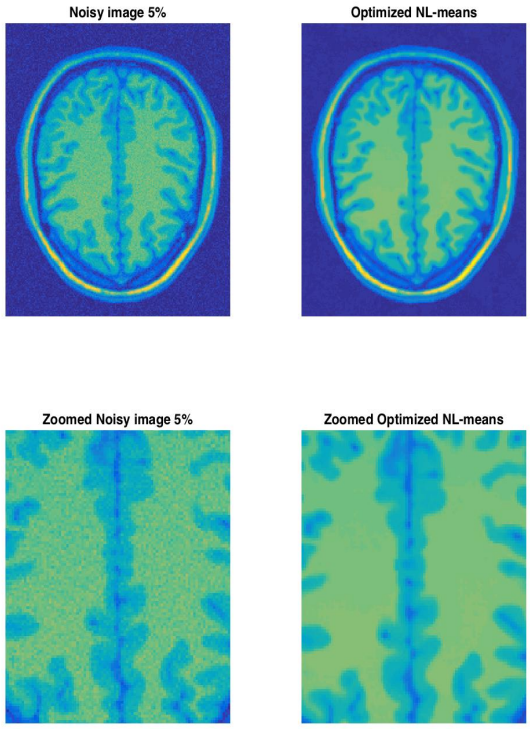

Figure 10 Noisy image with 5% noise added and its restoration, the image displayed is the slide 111th of the sequence.

4. T1 with ICBM protocol at 7% and 9% noise added :

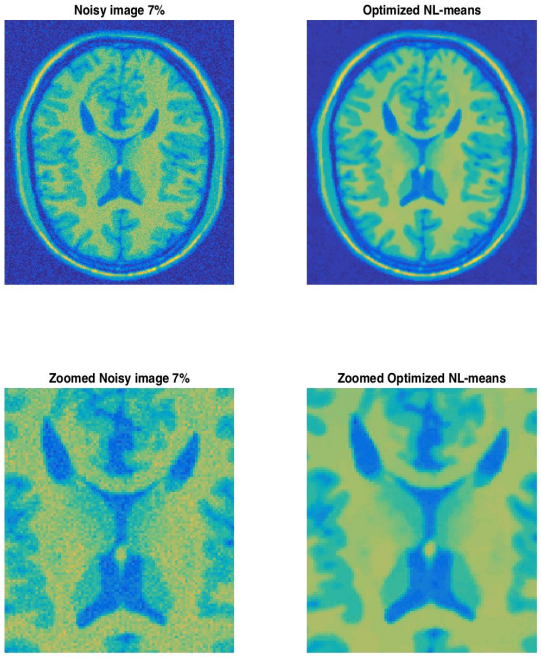

Figure 11 Noisy image with 7% noise added and its restoration, the image displayed is the slide 85th of the sequence.

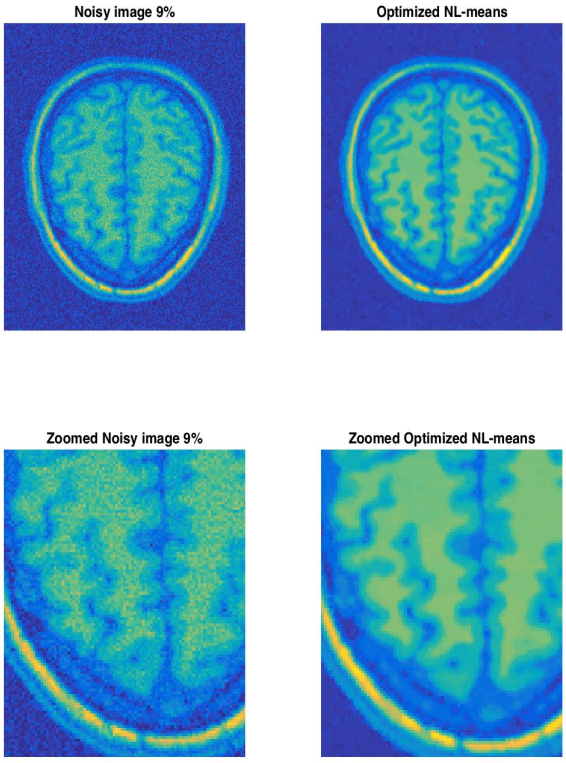

Figure 12 Noisy image with 9% noise added and its restoration, the image displayed is the slide 125th of the sequence.

5. T2 with AI protocol and MSL ground truth at all noise levels.

In this data set, we will see the power of filter in denoising image while preserve the small interest structure of brain. This dataset display MRI of a patient whose brain were damaged

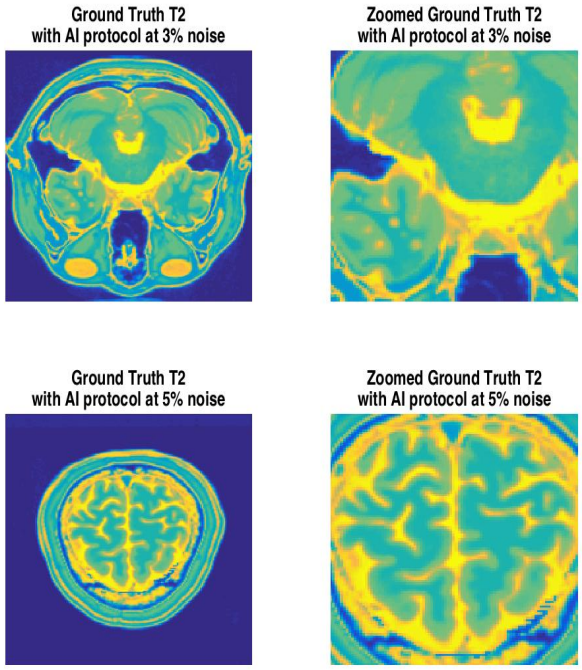

Figure 13 Ground truth of T2 with AI protocol at 3% and 5% noise added

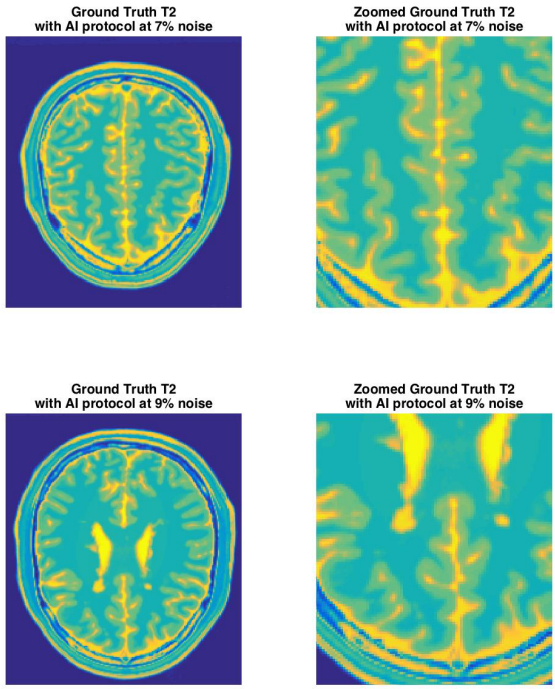

Figure 14 Ground truth of T2 with AI protocol at 7% and 9% noise added

6. **T2 with AI protocol and MSL at 3% and 5% noise added and its restorations**:

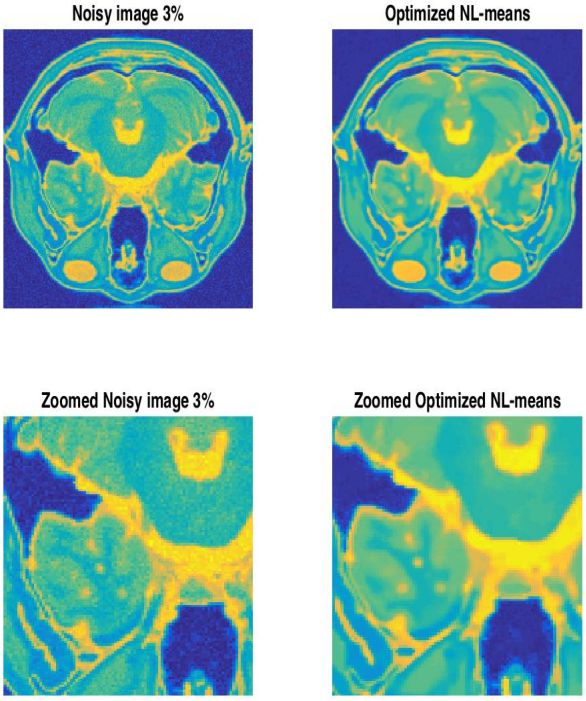

Figure 15 Noisy image with 3% noise added and its restoration, the image displayed is the slide 40th of the T2 sequence

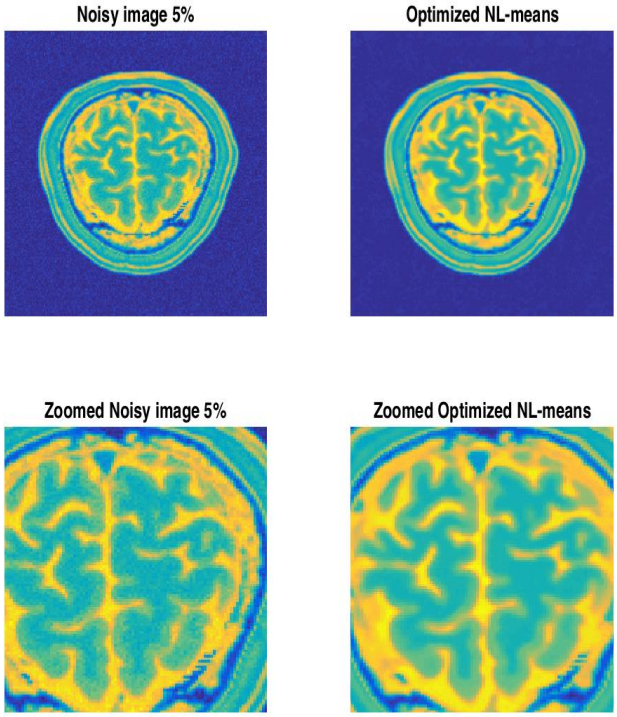

Figure 16 Noisy image with 5% noise added and its restoration, the image displayed is the slide 140 of the T2 sequence

7. **T2 with AI protocol and MSL at 7% and 9% noise added and its restorations:**

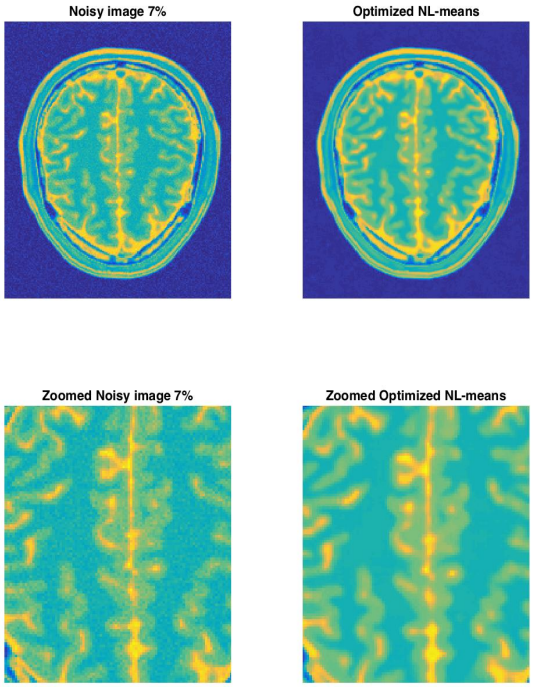

Figure 17 Noisy image with 7% noise added and its restoration, the image displayed is the slide 120 of the T2 sequence

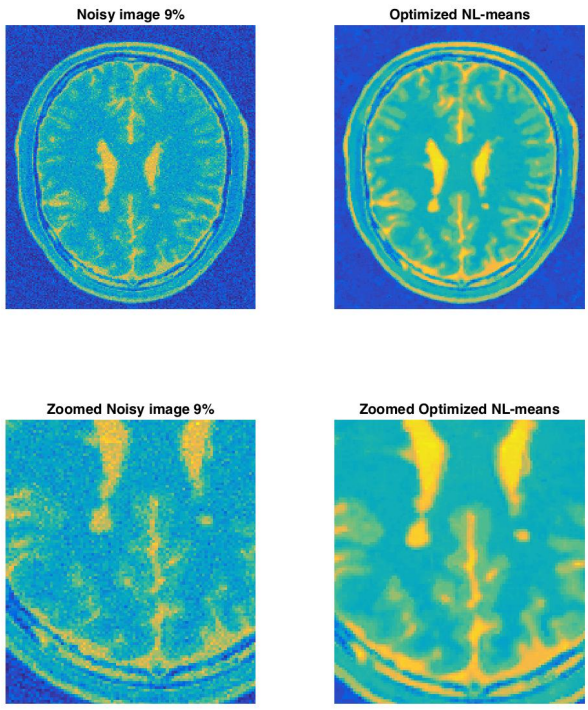

Figure 18 Noisy image with 9% noise added and its restoration, the image displayed is the slide 100th of the T2 sequence

VI. Discussion and Conclusion

In conclusion, this report has implemented the optimized NL means filter on the 3-D medical data. Several testing cases have been conducted on the BrainWeb dataset [2] and showed that the proposed filter works very well with different noise conditions and is able to tune the smoothing parameter to achieve better performance in different image contexts. Moreover, the novel method of selecting the critical voxel in searching volume has reduced the computational time of filtering images. Further work should be trying to implement the filter in parallel block-wise nonlocal means filter using a multicore machine to further speed up the computational time.

References

[1] A. Buades, B. Coll, and J. M. Morel, "A review of image denoising algorithms, with a new one," *Multiscale Model. Simul.*, vol. 4, no. 2, pp. 490–530, 2005.

[2] D. L. Collins, A. P. Zijdenbos, V. Kollokian, J. G. Sled, N. J. Kabani, C. J. Holmes, and A. C. Evans, "Design and construction of a realistic digital brain phantom," *IEEE Trans. Med. Imag.*, vol. 17, no. 3, pp. 463–468, Jun. 1998.

[3] P. Perona and J. Malik, "Scale-space and edge detection using anisotropic diffusion," *IEEE Trans. Pattern Anal. Mach. Intell.*, vol. 12, no. 7, pp. 629–639, Jul. 1990.

[4] L. I. Rudin, S. Osher, and E. Fatemi, "Nonlinear total variation based noise removal algorithms," *Physica D*, vol. 60, pp. 259–268, 1992.

[7] S. Geman and D. Geman, "Stochastic relaxation, Gibbs distribution, and the Bayesian restoration of images," *IEEE Trans. Pattern Anal. Mach. Intell.*, vol. 6, pp. 721–741, 1984.

[8] D. Mumford and J. Shah, "Optimal approximations by piecewise smooth functions and variational problems," *Commun. Pure Appl. Math.*, vol. 42, pp. 577–685, 1989.

[9] D. Tschumperlé,"Curvature-preserving regularization of multi-valued images using PDE's," in *ECCV*, Graz, Austria, 2006, pp. 428–433.

[10] M. J. Black and G. Sapiro, "Edges as outliers: Anisotropic smoothing using local image statistics," in *Proc. Scale-Space Theories Computer Vision*, Corfu, Greece, Sep. 1999, pp. 259–270.

[11] P. Saint-Marc, J.-S. Chen, and G. Medioni, "Adaptive smoothing: A general tool for early vision," *IEEE Trans. Pattern Anal. Mach. Intell.*, vol. 13, no. 6, pp. 514–529, Jun. 1991.

[12] D. L. Donoho and I. M. Johnstone, "Ideal spatial adaptation by wavelet shrinkage," *Biometrika*, vol. 81, no. 3, pp. 425–455, 1994.

[13] D. L. Donoho, "De-noising by soft-thresholding," *IEEE Trans. Inf. Theory*, vol. 41, no. 3, pp. 613–627, May 1995.

[14] J. PortillaandE.P.Simoncelli,"Image restoration using Gaussian scale mixtures in the wavelet domain," in *Int. Conf. Image Process.*, 2003, pp. 965–968.

[30] S. C. Zhu, Y. Wu, and D. Mumford, "Filters, random fields and maximum entropy (frame): Towards a unified theory for texture modeling," *Int. J. Comput. Vis.*, vol. 27, no. 2, pp. 107–126, 1998.

[31] W. T. Freeman, E. C. Pasztor, and O. T. Carmichael, "Learning low-level vision," *Int. J. Comput. Vis.*, vol. 40, no. 1, pp. 25–47, Oct. 2000.

[32] S. Roth and M. J. Black, "Fields of experts: A framework for learning image priors," in *2005 IEEE Comput. Soc. Conf. Computer Vision Pat- tern Recognit.*, San Diego, CA, Jun. 2005, pp. 860–867.

[34] G. Gerig, R. Kikinis, O. Kübler, and F. Jolesz, "Nonlinear anisotropic filtering of MRI data," *IEEE Trans. Med. Imag.*, vol. 11, no. 2, pp. 221–232, Jun. 1992.

[35] J. Weickert, B. M. ter Haar Romeny, and M. A. Viergever, "Efficient and reliable schemes for nonlinear diffusion filtering," *IEEE Trans. Image Process.*, vol. 7, no. 3, pp. 398–410, Jul. 1998.

[36] S. L. Keeling, "Total variation based convex filters for medical imaging," *Appl. Math. Comput.*, vol. 139, no. 1, pp. 101–119, 2003.

[37] W. C. K. Wong, A. C. S. Chung, and S. C. H. Yu, Trilateral filtering for biomedical images Arlington, VA, Apr. 2004, pp. 820–823.

[38] R. Nowak, "Wavelet-based Rician noise removal for magnetic resonance imaging," *IEEE Trans. Image Process.*, vol. 8, no. 10, pp. 1408–1419, Oct. 1999.

[39] J.C.WoodandK.M.Johnson,"Wavelet packet denoising of magnetic resonance images: Importance of Rician noise at low SNR," *Magn. Reson. Med.*, vol. 41, no. 3, pp. 631–635, Mar. 1999.

[40] S. Zaroubi and G. Goelman, "Complex denoising of MR data via wavelet analysis: Application for functional MRI," *Magn. Reson. Imag.*, vol. 18, no. 1, pp. 59–68, Jan. 2000.

[41] M. E. Alexander, R. Baumgartner, A. R. Summers, C. Windischberger, M. Klarhoefer, E. Moser, and R. L. Somorjai, "A wavelet-based method for improving signal-to-noise ratio and contrast in MR images," *Magn. Reson. Imag.*, vol. 18, no. 2, pp. 169–180, Feb. 2000.

[42] P. Bao and L. Zhang, "Noise reduction for magnetic resonance im- ages via adaptive multiscale products thresholding," *IEEE Trans. Med. Imag.*, vol. 22, no. 9, pp. 1089–1099, Sep. 2003.

[43] A. Ogier, P. Hellier, and C. Barillot, "Restoration of 3-D medical images with total variation scheme on wavelet domains (TVW)," in *Proc. SPIE Med. Imag. 2006: Image Process.*, San Diego, Feb. 2006.

[44] Y. Wang and H. Zhou, "Total variation wavelet-based medical image denoising," *Int. J. Biomed. Imag.*, vol. 2006, 2006.

[45] M. J. McDonnell, "Box-filtering techniques," *Comput. Vis., Graph., Image Process.*, vol. 17, no. 1, pp. 65–70, Sep. 1981.

[49] T. Gasser, L. Sroka, and C. J. Steinmetz, "Residual variance and residual pattern in nonlinear regression," *Biometrika*, vol. 73, no. 3, pp. 625–633, 1986.

[50] J. Boulanger, C. Kervrann, and P. Bouthemy, "Adaptive spatio-temporal restoration for 4D fluoresence microscopic imaging," presented at the Int. Conf. Medical Image Comput. Computer Assisted Interven- tion (MICCAI' 05), Palm Springs, CA, Oct. 2005.

[51] A. Buades, B. Coll, and J.-M. Morel, "Nonlocal image and movie denoising," *Int. J. Comput. Vis.*, vol. 76, no. 2, pp. 123–140, 2008.

[52] M. Mahmoudi and G. Sapiro, "Fast image and video denoising via nonlocal means of similar neighborhoods," *IEEE Signal Process. Lett.*, vol. 12, no. 12, pp. 839–842, Dec. 2005.